Numerical Simulation of the full 1st order Post Newtonian Corrections for the GPS and GLONASS satellites

Kyoung-Min Roh, Sung-Moon Yoo, Byung-Kyu Choi, and Jung-Ho Cho
Space Geodesy Group, *Korea Astronomy and Space Science Institute*

Abstract

Our main motivation in this work was to investigate the effects of the full set of first order PN perturbations on the GNSS orbits, specifically on the GPS and the GLONASS orbits. In this study, the full 1st PN corrections are first implemented in a high-fidelity orbit propagation software, KASIOP (Korea Astronomy and Space Science Institute Orbit Propagator). In most SW, the only three relativistic perturbations i.e., the Schwarzschild term, Lense-Thirring effect, and the geodesic precession are considered and the other small terms are ignored without any numerical evaluation. In this study, the effects of the full 1st PN corrections are evaluated through extensive numerical simulations. The results presented in this study can be useful to define the magnitudes of the PN corrections for their use in future.

Background and Simulation Scope

A.Post-Newtonian Equations of Motion

The general theory of relativity (GR) deals with gravity. Spacetime around a body with a certain mass is curved, and gravity can be thought of as a curvature of spacetime in GR. Namely, the geometry of spacetime, described mathematically using a metric tensor, defines the motion of a particle in the spacetime continuum. Resolution B1.3 of 2000 adopted by the International Astronomical Union (IAU) states the relativistic reference frames based on the metric tensors defined for the geocentric and barycentric coordinates, i.e., the Geocentric Celestial Reference System (GCRS) and the Barycentric Celestial Reference System (BCRS). Using the geocentric metric tensor, the PN equations of motion of a near-Earth satellite can be formulated using the geodesic equation of motion. The formulas derived by Brumberg and Kopejkin [1] were used in this study. The resultant equations of motion are as follows

$$\frac{d^2\hat{\boldsymbol{r}}}{d\hat{t}^2} = \boldsymbol{a}_N + \boldsymbol{a}_{NC} + \frac{1}{c^2}\sum_{i=1}^{7}\boldsymbol{\Phi}_i$$

where $(\hat{\boldsymbol{r}}, \hat{t})$ is the geocentric coordinate and time, $\boldsymbol{a}_N$ is the Newtonian acceleration vector, $\boldsymbol{a}_{NC}$ is the acceleration due to non-conservative forces (such as the radiation pressures from the Sun and the Earth), and $\boldsymbol{\Phi}_i$ are the 1st PN perturbations. In this article, $\boldsymbol{\Phi}_i$ were divided into seven accelerations.

- **Schwarzschild term** : $\boldsymbol{\Phi}_1 = \frac{G\hat{M}_E}{|\hat{\boldsymbol{r}}|^3}\left[\left(\frac{4G\hat{M}_E}{|\hat{\boldsymbol{r}}|} - \hat{v}^2\right)\hat{\boldsymbol{r}} + 4(\hat{\boldsymbol{r}}\cdot\hat{\boldsymbol{v}})\hat{\boldsymbol{v}}\right]$

- **Lense-Thirring effect** : $\boldsymbol{\Phi}_2 = \frac{2G}{|\hat{\boldsymbol{r}}|^3}C\hat{\omega}\left[\hat{\boldsymbol{v}}\times\boldsymbol{s} + \frac{3\hat{\boldsymbol{r}}}{|\hat{\boldsymbol{r}}|^2}(\hat{\boldsymbol{r}}\times\hat{\boldsymbol{v}})\right]$

- **Relativistic effect due to the Earth quadrupole moment**

$$\boldsymbol{\Phi}_3 = \frac{4G^2\hat{M}_E}{|\hat{\boldsymbol{r}}|^6}\left\{-2\mathrm{diag}(\boldsymbol{I}_E)\hat{\boldsymbol{r}} - 3\boldsymbol{I}_E\hat{\boldsymbol{r}} + \frac{9}{|\hat{\boldsymbol{r}}|^2}[(\boldsymbol{I}_E\hat{\boldsymbol{r}})^T\cdot\hat{\boldsymbol{r}}]\hat{\boldsymbol{r}}\right\} + \frac{3}{2}\frac{G}{|\hat{\boldsymbol{r}}|^5}\hat{v}^2\left\{\mathrm{diag}(\boldsymbol{I}_E) + 2\boldsymbol{I}_E\hat{\boldsymbol{r}} - \frac{5}{|\hat{\boldsymbol{r}}|^2}[(\boldsymbol{I}_E\hat{\boldsymbol{r}})^T\cdot\hat{\boldsymbol{r}}]\hat{\boldsymbol{r}}\right\} + 6\frac{G}{|\hat{\boldsymbol{r}}|^5}\hat{\boldsymbol{v}}\left\{-\mathrm{diag}(I_E)(\hat{\boldsymbol{r}}\cdot\hat{\boldsymbol{v}}) - 2[(\boldsymbol{I}_E\hat{\boldsymbol{v}})^T\cdot\hat{\boldsymbol{r}}] + \frac{5}{|\hat{\boldsymbol{r}}|^2}[(\boldsymbol{I}_E\hat{\boldsymbol{r}})^T\cdot\hat{\boldsymbol{r}}](\hat{\boldsymbol{r}}\cdot\hat{\boldsymbol{v}})\right\}$$

- **Nonlinear coupling of the monopole of the Earth and the gravitoelectric tidal filed**

$$\boldsymbol{\Phi}_4 = -4\frac{G\hat{M}_E}{|\hat{\boldsymbol{r}}|}\,\bar{\boldsymbol{U}}_D\cdot\hat{\boldsymbol{r}} + 2\frac{GM_E}{|\hat{\boldsymbol{r}}|^3}[(\bar{\boldsymbol{U}}_D\hat{\boldsymbol{r}})^T\cdot\hat{\boldsymbol{r}}]\hat{\boldsymbol{r}}$$

- **Gravitomagnetic component of the tidal perturbation**

$$\boldsymbol{\Phi}_5 = -4[(\bar{\boldsymbol{U}}_D\hat{\boldsymbol{v}})^T\cdot\hat{\boldsymbol{r}}]\hat{\boldsymbol{v}} + |\hat{\boldsymbol{v}}|^2\bar{\boldsymbol{U}}_D\hat{\boldsymbol{r}} + 4\begin{bmatrix}(\bar{\boldsymbol{V}}_D^1\hat{\boldsymbol{v}})^T\cdot\hat{\boldsymbol{r}}\\(\bar{\boldsymbol{V}}_D^2\hat{\boldsymbol{v}})^T\cdot\hat{\boldsymbol{r}}\\(\bar{\boldsymbol{V}}_D^3\hat{\boldsymbol{v}})^T\cdot\hat{\boldsymbol{r}}\end{bmatrix} + 4\begin{bmatrix}(\bar{\boldsymbol{V}}_{1D}\hat{\boldsymbol{r}})^T\cdot\hat{\boldsymbol{v}}\\(\bar{\boldsymbol{V}}_{2D}\hat{\boldsymbol{r}})^T\cdot\hat{\boldsymbol{v}}\\(\bar{\boldsymbol{V}}_{3D}\hat{\boldsymbol{r}})^T\cdot\hat{\boldsymbol{v}}\end{bmatrix} - 4[(\bar{\boldsymbol{U}}_D\hat{\boldsymbol{v}})^T\cdot\hat{\boldsymbol{r}}]\boldsymbol{v}_E + 4(\boldsymbol{v}_E\cdot\hat{\boldsymbol{v}})(\bar{\boldsymbol{U}}_D\hat{\boldsymbol{r}}) + 2(\dot{\boldsymbol{a}}_E\cdot\hat{\boldsymbol{v}})\hat{\boldsymbol{r}} - 2(\hat{\boldsymbol{r}}\cdot\hat{\boldsymbol{v}})\dot{\boldsymbol{a}}_E$$

- **Gravitoelectric component of the tidal perturbation**

$$\boldsymbol{\Phi}_6 = \boldsymbol{F}[(\bar{U}_D)^T\boldsymbol{r}_E] + \bar{\boldsymbol{U}}_D(\boldsymbol{F}^T\hat{\boldsymbol{r}}) - 4\begin{bmatrix}(\bar{\boldsymbol{V}}_{1D}\hat{\boldsymbol{r}})^T\cdot\boldsymbol{v}_E\\(\bar{\boldsymbol{V}}_{2D}\hat{\boldsymbol{r}})^T\cdot\boldsymbol{v}_E\\(\bar{\boldsymbol{V}}_{3D}\hat{\boldsymbol{r}})^T\cdot\boldsymbol{v}_E\end{bmatrix} + 2v_E^2(\bar{\boldsymbol{U}}_D\hat{\boldsymbol{r}}) - 2\bar{U}(\bar{\boldsymbol{U}}_D\hat{\boldsymbol{r}}) - \frac{1}{2}\boldsymbol{v}_E[(\bar{\boldsymbol{U}}_D\hat{\boldsymbol{v}})\cdot\hat{\boldsymbol{r}}] - \frac{1}{2}(\bar{\boldsymbol{U}}_D\boldsymbol{v}_E)(\boldsymbol{v}_E\cdot\hat{\boldsymbol{r}}) + \bar{\boldsymbol{W}}_D\hat{r} + \ddot{\bar{U}}\hat{r} + 2\left(\frac{\partial\dot{\bar{V}}}{\partial\hat{r}}\right)\hat{\boldsymbol{r}} + 2\left(\frac{\partial\dot{\bar{V}}}{\partial\hat{r}}\right)^T\hat{\boldsymbol{r}} - 3\boldsymbol{a}_E(\boldsymbol{a}_E\cdot\hat{\boldsymbol{r}}) - \boldsymbol{v}_E(\dot{\boldsymbol{a}}_E\cdot\hat{\boldsymbol{r}}) - (\hat{\boldsymbol{r}}\cdot\boldsymbol{v}_E)\dot{\boldsymbol{a}}_E$$

- **Geodesic precession**

$$\boldsymbol{\Phi}_7 = 3\left\{\dot{\boldsymbol{r}}_{ES}\times\left(-\frac{GM_S\boldsymbol{r}_{ES}}{c^2r_{ES}^3}\right)\right\}\times\hat{\boldsymbol{v}}$$

*The details of the terms inside the above equations can be found in Ref. [2].

B. Scope of the Numerical Simulation

The numerical simulations of the effect of these first-order PN corrections were conducted for the GPS and the GLONASS systems. In this study, five orbits were selected with different ascending nodes and different body types. The orbital elements (IGS final orbit) and the body models of the studied satellites in here are summarized in Table 1.

Table 1. Orbital elements and body types of the tested GNSS satellites (Jan. 1, 2016)

	GPS-01	GPS-02	GPS-05	GLONASS-01	GLONASS-25
Body Model	BLOCK IIF	BLOCK IIR-B	BLOCK IIR-M	GLONASS-M	GLONASS-K1
$a\ (km)$	26558.614	26559.232	26562.4368	25506.554	25509.582
e	0.00493390	0.01522123	0.00464273	0.00040069	0.00072658
$i\ (°)$	55.289	54.073	54.198	64.128	65.258
$\Omega\ (°)$	121.702	119.395	180.865	201.5904	82.512
$\omega\ (°)$	27.344	234.448	27.744	26.489	218.694

The PN corrections are implemented to a high-precision orbit propagation software for realistic simulations, i.e., KASIOP package that was developed by the KASI. The reference coordinates and time for the numerical integration of the equations of motion of the studied satellites were set to the Earth-centered International Celestial Reference System (ICRS), also known as J2000.0 and Terrestrial Time (TT), respectively. The included perturbations and therein space environment models, and the numerical methods such as integration and interpolation, are listed in Table 2.

Continue …

Table 2. Lists of the Models applied to the orbit propagation

Item	Applied Model
Geopotential	
Zero-tide geopotential	EGM 2008, 70 × 70
Solid Earth/Solid Earth Pole/Ocean Pole Tide	IERS Convections (2010)
Ocean Tide	FES 2004
Earth Rotation	
Precession-Nutation	IAU 2006/2000
Earth Rotation Parameters	IERS ERP C04
Numerical Method	
Integration	10th order Summed Adams–Bashforth–Moulton, 60s of the step size
Interpolation	10th order Lagrangian
Space Environments	
Atmospheric density	JB2008
Earth Radiation	Rodrigues–Solano et al.
Solar system ephemeris	INPOP 13c
Spacecraft Body	
Box-Wing Model	Rodrigues–Solano et al.

Results

A. Comparison of the perturbations

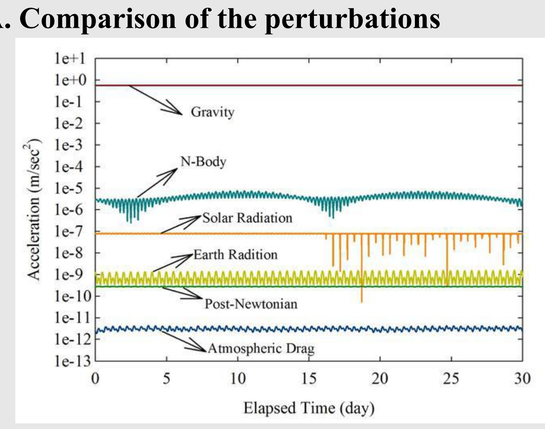

Fig. 1. Accelerations of GPS PRN01

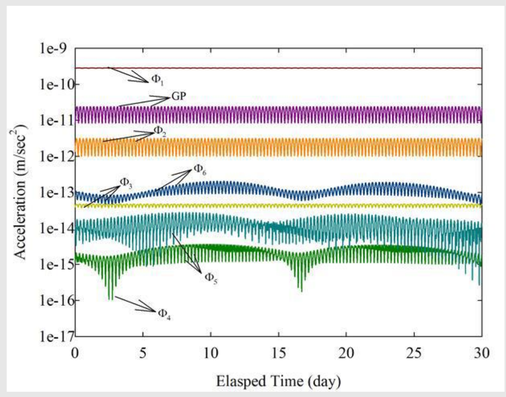

Fig. 2. Accelerations of the PN perturbations for GPS PRN01

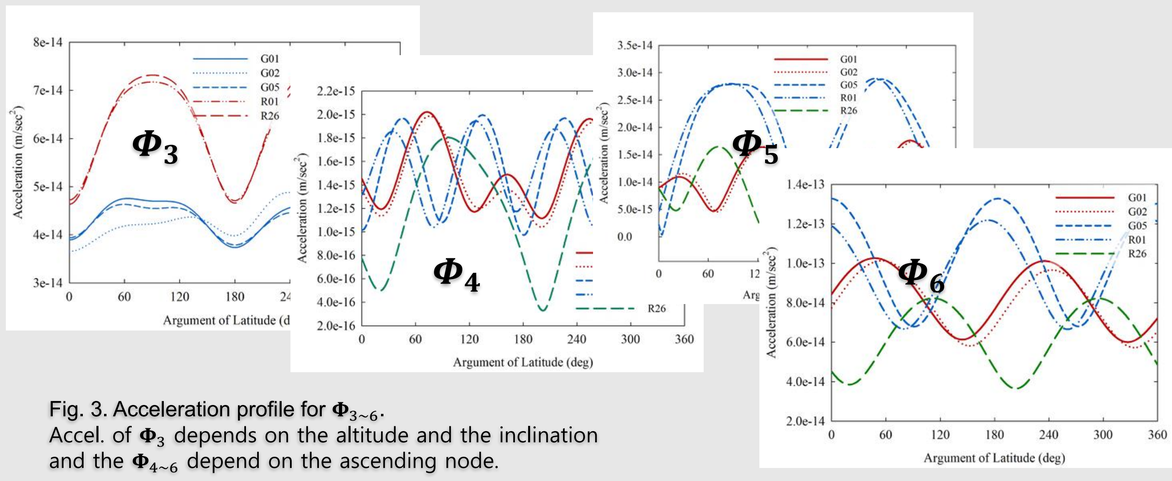

Fig. 3. Acceleration profile for $\boldsymbol{\Phi}_{3\sim6}$.
Accel. of $\boldsymbol{\Phi}_3$ depends on the altitude and the inclination and the $\boldsymbol{\Phi}_{4\sim6}$ depend on the ascending node.

B. Compare two orbits with and w/o a specific PN term

By performing this test, we estimated the effects of specific PN terms as well as the cumulative effect.

Case 1: $(\boldsymbol{a}_N + \boldsymbol{a}_{NC} + \boldsymbol{\Phi}_1) - (\boldsymbol{a}_N + \boldsymbol{a}_{NC})$
Case 2: $(\boldsymbol{a}_N + \boldsymbol{a}_{NC} + \boldsymbol{\Phi}_1 + \boldsymbol{\Phi}_{GP}) - (\boldsymbol{a}_N + \boldsymbol{a}_{NC} + \boldsymbol{\Phi}_1)$
Case 3: $(\boldsymbol{a}_N + \boldsymbol{a}_{NC} + \boldsymbol{\Phi}_1 + \boldsymbol{\Phi}_{GP} + \boldsymbol{\Phi}_2) - (\boldsymbol{a}_N + \boldsymbol{a}_{NC} + \boldsymbol{\Phi}_1 + \boldsymbol{\Phi}_{GP})$
Case 4: $(\boldsymbol{a}_N + \boldsymbol{a}_{NC} + \boldsymbol{\Phi}_1 + \boldsymbol{\Phi}_{GP} + \boldsymbol{\Phi}_2 + \boldsymbol{\Phi}_6) - (\boldsymbol{a}_N + \boldsymbol{a}_{NC} + \boldsymbol{\Phi}_1 + \boldsymbol{\Phi}_{GP} + \boldsymbol{\Phi}_2)$
Case 5: $(\boldsymbol{a}_N + \boldsymbol{a}_{NC} + \boldsymbol{\Phi}_1 + \boldsymbol{\Phi}_{GP} + \boldsymbol{\Phi}_2 + \boldsymbol{\Phi}_6 + \boldsymbol{\Phi}_3) - (\boldsymbol{a}_N + \boldsymbol{a}_{NC} + \boldsymbol{\Phi}_1 + \boldsymbol{\Phi}_{GP} + \boldsymbol{\Phi}_2 + \boldsymbol{\Phi}_6)$
Case 6: $(\boldsymbol{a}_N + \boldsymbol{a}_{NC} + \boldsymbol{\Phi}_1 + \boldsymbol{\Phi}_{GP} + \boldsymbol{\Phi}_2 + \boldsymbol{\Phi}_6 + \boldsymbol{\Phi}_3 + \boldsymbol{\Phi}_5) - (\boldsymbol{a}_N + \boldsymbol{a}_{NC} + \boldsymbol{\Phi}_1 + \boldsymbol{\Phi}_{GP} + \boldsymbol{\Phi}_2 + \boldsymbol{\Phi}_6 + \boldsymbol{\Phi}_3)$
Case 7: $(\boldsymbol{a}_N + \boldsymbol{a}_{NC} + \boldsymbol{\Phi}_1 + \boldsymbol{\Phi}_{GP} + \boldsymbol{\Phi}_2 + \boldsymbol{\Phi}_6 + \boldsymbol{\Phi}_3 + \boldsymbol{\Phi}_5 + \boldsymbol{\Phi}_4) - \left(\boldsymbol{a}_N + \boldsymbol{a}_{NC} + \sum_{i=1}^{7}\boldsymbol{\Phi}_i\right)$

Table 3. Effects of the different PN corrections on the satellite (PRN01) position

	Max. Radial(mm)	Max. Along (mm)	Max. Cross (mm)	Max. Pos. (mm)
Case 1 (w/wo Φ_1)	35.38	2289.66	0.05	2289.93
Case 2 (w/wo Φ_{GP})	0.89	69.58	46.69	83.80
Case 3 (w/wo Φ_2)	0.10	8.37	6.14	10.38
Case 4 (w/wo Φ_6)	0.01	0.34	0.14	0.36
Case 5 (w/wo Φ_3)	0.0	0.21	0.05	0.21
Case 6 (w/wo Φ_5)	0.02	0.08	0.00	0.08
Case 7 (w/wo Φ_4)	0.0	0.01	0.00	0.01

Conclusion

Advances in atomic clocks, which is one of key technologies in a GNSS, promote the role of the GNSS in space geodesy. Therefore, there is a growing need for more accurate modeling of the equations of motion of GNSS satellites and better measurement equations. In this study, the effects of the full set of 1st PN perturbations on the GPS and GLONASS satellites are investigated by conducting realistic simulations. Beside the perturbations $\boldsymbol{\Phi}_{1,2,7}$ which are listed in IERS Conventions, the other PN perturbations are still very small and can be considered as ignorable terms at this moments. However, the results presented in this study can be useful to define the magnitudes of the PN corrections and also for their use in future.

Reference

[1] Brumberg VA, Kopejkin SM (1989) Relativistic reference systems and motion of test bodies in the vicinity of the Earth. Nuovo Cim 103:63–98.
[2] Roh, K.-M., Kopeikin, S. M., and Cho, J.-H., "Numerical simulation of the post-Newtonian equations of motion for the near Earth satellite with an application to the LARES satellite," *Adv. in Space Research*, 58 (11), 2016